Electronic Supplementary Material (ESI) for Journal of Materials Chemistry C
This journal is © The Royal Society of Chemistry 2013

Quantitative X-ray Absorption and Emission Spectroscopies: Electronic Structure Elucidation of Cu_2S and CuS

Prashant Kumar,[1] Rajamani Nagarajan,[1] Ritimukta Sarangi[2,]*

[1]Materials Chemistry Group, Department of Chemistry, University of Delhi, Delhi, India, 110007

[2]Stanford Synchrotron Radiation Laboratory, SLAC National Accelerator Laboratory, Menlo Park, CA 94025, USA

*Corresponding authors: ritis@slac.stanford.edu

This journal is © The Royal Society of Chemistry 2013

Cu K-edge EXAFS

The non-phase shift corrected Fourier Transforms (FT) of the Cu K-edge EXAFS for Cu_2S and CuS are presented in Figure S1A and S1B, respectively, along with their FEFF fits. The inset shows the corresponding EXAFS region. There is a significant change in EXAFS intensity between the two complexes, with CuS being more intense than Cu_2S. FT data for Cu_2S show two peaks at 1.83 Å and 2.31 Å and that for CuS show two peaks at 1.80 Å and 3.45 Å. The Cu K-edge EXAFS data for both Cu_2S and CuS have been reported in the literature but show significant variability and are of poorer resolution as inferred from the FT data. Most importantly, the reported EXAFS for CuS has only the first shell peak, the peak at 3.45 Å is either completely missing or is dramatically diminished. Since Cu is extremely concentrated in these samples, the lack of longer distance features and the poor resolution likely indicates self-absorption problems brought about by suboptimal sample to BN ratio. FEFF fits to the EXAFS data are presented in Table S1 and are in reasonably good agreement with the crystal structures of covellite and low-chalcocite, indicating that the samples are pure and have not undergone oxidation.

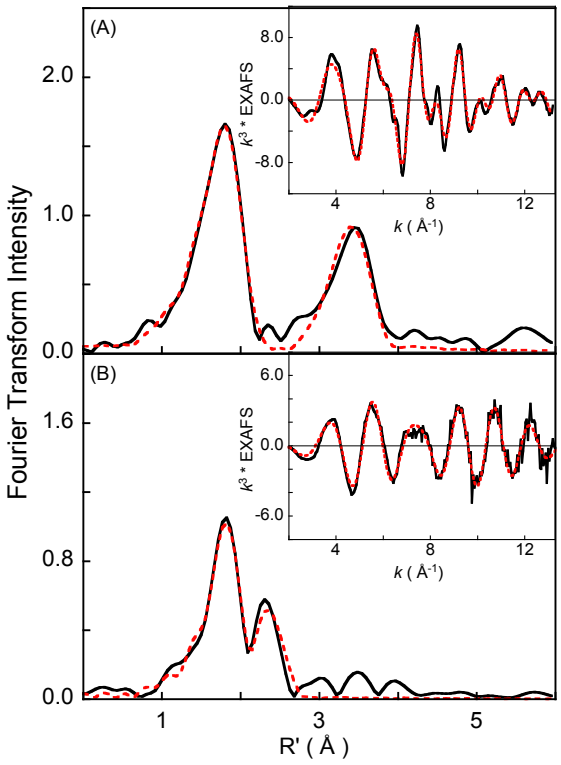

Figure S1 Non-phase shift corrected Fourier transform data for (A) CuS and (B) Cu_2S. The inset show the corresponding EXAFS region. Data are represented with solid black curves. FEFF fits are represented with dashed red curves.

This journal is © The Royal Society of Chemistry 2013

Cu K-edge XAS

The data presented in Figure 1 in the main manuscript are qualitatively similar to those present in the literature, however quantitative differences can be observed. First, the data in the literature have some variability in the edge-region, indicating either contamination (likely arising due to surface oxidation) or self-absorption. Second, the data presented here have sharper rising-edge features (clearly observed for CuS) indicating higher resolution and minimal self-absorption. The effect of self-absorption in both the rising-edge and EXAFS region is dramatic and is demonstrated with CuS as an example in Figure S2.

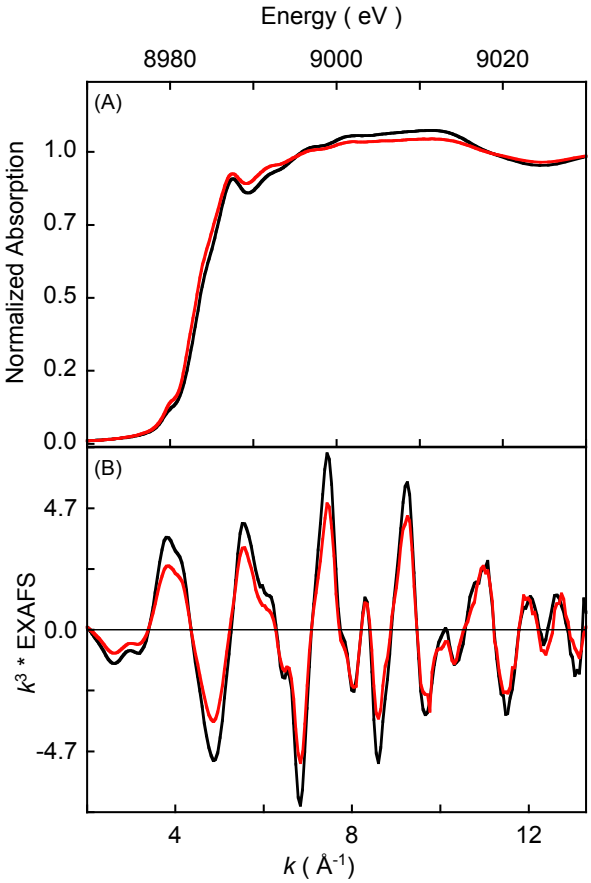

Figure S2 Cu K-edge XAS (A) and EXAFS (B) data for CuS obtained on samples prepared with different BN:CuS ratio (by weight). BN is used to dilute the sample to prevent self-absorption. For the black and red spectra BN:CuS was 10:1 and 5:1, respectively.

This journal is © The Royal Society of Chemistry 2013

Density Functional Theory

To predict the X-ray emission spectra (Kβ" region), simplistic models of Cu^{2+}-sulfide (2-atom) and Cu^{2+}-disulfide (3-atom) were created. Gradient-corrected, (GGA) spin-unrestricted density functional theory (DFT) calculations were carried out using ORCA[1,2] on a 8-cpu cluster. The Becke[3,4] exchange and the Perdew[5] correlational functional was used. Ahlrichs' triple-ζ valence basis set[6,7] with polarization functions (TZVP) was used on the S atoms and the core properties CP(PPP)[8] basis set (as implemented in ORCA) was used on Cu. Conductor like solvation model[9] and tight convergence criterion were used on all calculations. The calculated energies and intensities were Gaussian broadened with half-widths of 1.5 eV to account for core-hole lifetime and instrument resolution. The XES spectra were calculated using literature protocol.[10,11] The calculated $K\beta_{1,3}$ and Kβ" spectra for Cu^{2+}-monosulfide $(S)^{2-}$ and Cu^{2+}-disulfide (S_2^{2-}) are shown in Figure S3.

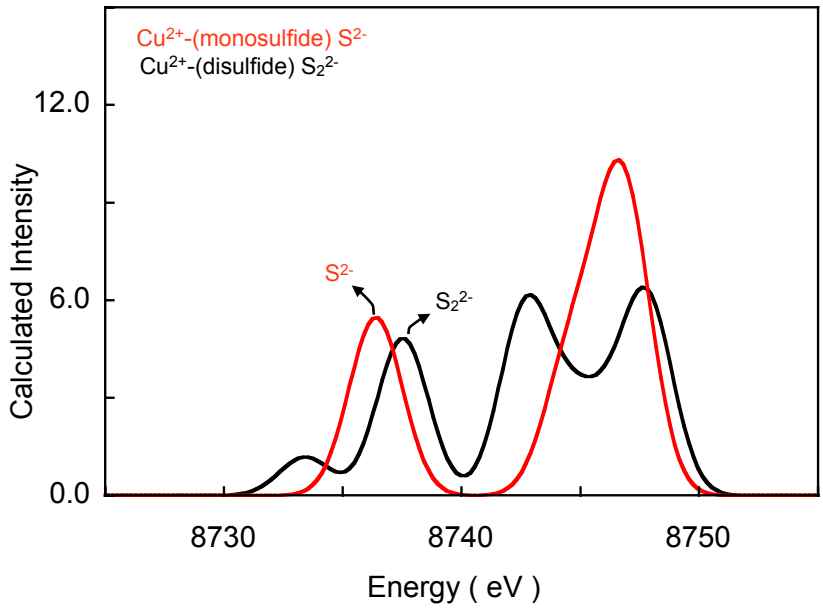

Figure S3 TD-DFT calculated $K\beta_{1,3}$ and Kβ" data. The calculated energies are 227 eV down shifted relative to the experimental energies. This is generally the case with core level TD-DFT calculations since DFT does not describe core potentials accurately, resulting in the core levels being too high in energy relative to the valence levels.

This journal is © The Royal Society of Chemistry 2013

Cu L-edge XAS of CuS

Cu L-edge XAS data for CuS were taken from literature. CuS has a low-energy features at ~931.7 eV (recalibrated for comparison to discreet molecular system presented here). Two arguments have been made about this feature: first that this feature falls in the range of Cu(I) complexes (931.9 – 933.4 eV)[12] and second that Cu L-edge data for Cu(II) complexes are ~25 times more intense than Cu(I) complexes.[13,14] Both arguments are correct for Cu bonded to light atom ligands. However, in the case of Cu-S compounds, two things happen, first, strong covalent overlap between the two leads to delocalization of the $3d^9$ hole onto the sulfur. This in turn, decreases the transition probability of Cu 2p to the now delocalized Cu 3d orbital. Second, due to increase in ligand field, the energy of the low-energy edge feature shifts to higher energy relative to light atom systems.[15] Comparison of the L-edge data for $[Cu(TMPA)(OH_2)](ClO_4)$[16] (5 Cu-N/O bonds) and $[(Cu[HB(3,5\text{-}Pr^i{}_2pz)_3)]_2(S_2)]$[15] (2 Cu-S and 3 Cu-N bonds) demonstrates these two effects (Figure S4). The data show a sharp decrease in intensity and an increase in energy position in Cu-S containing compounds. Therefore, even if the 2p→ 3d transitions are ~25 times[14] stronger than the 2p → 4s transitions in typical Cu^{2+} systems and far overwhelm the higher energy features in the XAS spectra, in Cu-S systems the 2p→ 3d transitions are of modest intensity.

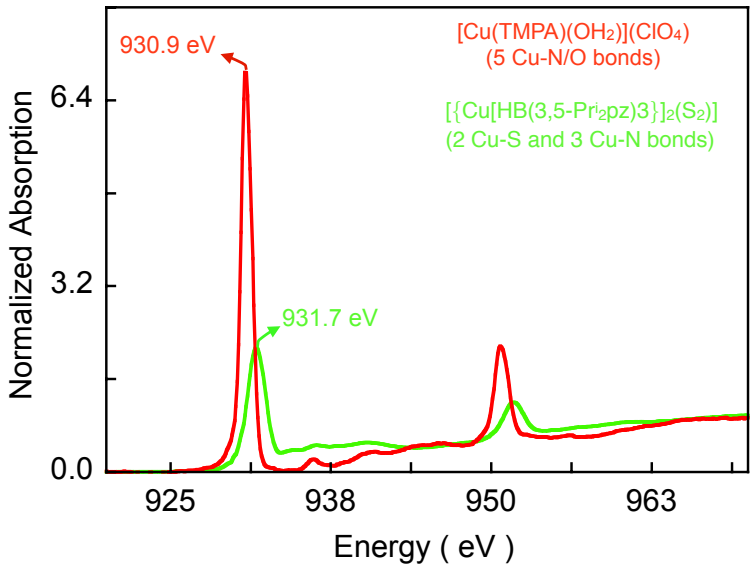

Figure S4 The normalized Cu L-edge XAS data for $[Cu(TMPA)(OH_2)](ClO_4)$ (—) and $[(Cu[HB(3,5\text{-}Pr^i{}_2pz)_3)]_2(S_2)]$ (—).

The comparison of Cu L-edge XAS spectra of $[(Cu[HB(3,5\text{-}Pr^{i}{}_{2}pz)_{3})]_{2}(S_{2})]$ and CuS[12](reproduced) shows that the CuS has transition similar in energy as the Cu^{2+} 2p → 3d transition in $[(Cu[HB(3,5\text{-}Pr^{i}{}_{2}pz)_{3})]_{2}(S_{2})]$. This peak is significantly diminished. This can be attributed to two factors: first, a stronger covalent interaction in CuS (3 Cu-S and 4 Cu-S interactions). Second, only a third of the Cu sites contribute to the pre-edge whereas the rest contribute only to the higher energy 2p → 4s transition. These two factors obscure the Cu^{2+} feature in the spectra of CuS and have led to the misinterpretation of electronic structure based on Cu L-edge XAS.

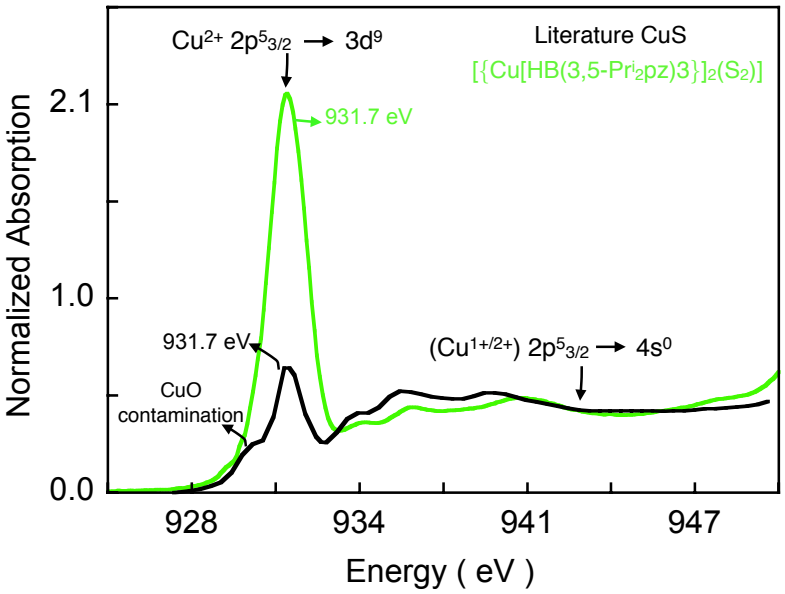

Figure S5 The normalized Cu L-edge XAS data for CuS (—) and $[(Cu[HB(3,5\text{-}Pr^{i}{}_{2}pz)_{3})]_{2}(S_{2})]$ (—).

This journal is © The Royal Society of Chemistry 2013

Table S1. EXAFS Least Squares Fit Parameters

	Coordination/Path	R (Å)[a]	σ^2 (Debye-Waller)	E_0	F^b
CuS	1 Cu-S	2.17	0.0070	-15.43	0.8
	3.3 Cu-S	2.9	0.0032		
	6 Cu-Cu	3.26	0.0260		
	6 Cu-Cu	3.78	0.0076		
Cu_2S	3 Cu-S	2.29	0.0072	-15.6	0.31
	2 Cu-Cu	2.72	0.0069		
	2 Cu-Cu	2.89	0.0063		

[a]The estimated standard deviations for the distances are in the order of ± 0.02 Å. [b]Error is given by $\Sigma[(\chi_{obsd} - \chi_{calcd})^2 k^6]/\Sigma[(\chi_{obsd})^2 k^6]$. The S_0^2 factor was set at 0.9.

This journal is © The Royal Society of Chemistry 2013

References

(1) Neese, F. *ORCA: An Ab initio, DFT and Semiempirical Electronic Structure Package*., Version 2.6.35, 2008.
(2) Neese, F.; Olbrich, G. *Chem. Phys. Lett.* **2002**, *362*, 170-178.
(3) Becke, A. D. *J. Chem. Phys.* **1993**, *98*, 5648-5652.
(4) Becke, A. D. *Phys. Rev. A* **1988**, *38*, 3098-3100.
(5) Perdew, J. P. *Phys. Rev. B* **1986**, *33*, 8822-8824.
(6) Schaefer, A.; Horn, H.; Ahlrichs, R. *J. Chem. Phys.* **1992**, *97*, 2571-2577.
(7) Schaefer, A.; Huber, C.; Ahlrichs, R. *J. Chem. Phys.* **1994**, *100*, 5829-5835.
(8) Sinnecker, S.; Slep, L. D.; Bill, E.; Neese, F. *Inorg. Chem.* **2005**, *44*, 2245-2254.
(9) Sinnecker, S.; Rajendran, A.; Klamt, A.; Diedenhofen, M.; Neese, F. *J. Phys. Chem. A* **2006**, *110*, 2235-2245.
(10) Lee, N.; Petrenko, T.; Bergmann, U.; Neese, F.; DeBeer, S. *J. Am. Chem. Soc.* **2010**, *132*, 9715-9727.
(11) Roemelt, M.; Beckwith, M. A.; Duboc, C.; Collomb, M. N.; Neese, F.; DeBeer, S. *Inorg. Chem.* **2012**, *51*, 680-687.
(12) Todd, E. C.; Sherman, D. M. *Amer. Min.* **2003**, *88*, 1652-1656.
(13) Pattrick, R. A. D.; van der Laan, G.; Vaughan, D. J.; Henderson, C. M. B. *Phys. Chem. Min.* **1993**, *20*., 395–401.
(14) Pattrick, R. A. D.; Mosselmans, J. F. W.; Charnock, J. M.; England, K. E. R.; Helz, G. R.; Garner, C. D.; Vaughan, D. J. *Geochim. Cosmochim. Acta* **1997**, *61*, 2023–2036.
(15) Sarangi, R.; York, J. T.; Helton, M. E.; Fujisawa, K.; Karlin, K. D.; Tolman, W. B.; Hodgson, K. O.; Hedman, B.; Solomon, E. I. *J. Am. Chem. Soc.* **2008**, *130*, 676-686.
(16) Sarangi, R.; Solomon, E. I. Unpublished Results.